UC Santa Barbara

UC Santa Barbara Previously Published Works

Title

Electric field-tunable BaxSr12xTiO3 films with high figures of merit grown by molecular beam epitaxy

Permalink

https://escholarship.org/uc/item/2n1712rg

Journal

Applied Physics Letters, 101(25)

Authors

Mikheev, Evgeny
Kajdos, Adam
Hauser, Adam
et al.

Publication Date

2012-12-21

Peer reviewed

eScholarship.org Powered by the California Digital Library
University of California

CrossMark click for updates

Electric field-tunable $Ba_xSr_{1-x}TiO_3$ films with high figures of merit grown by molecular beam epitaxy

Evgeny Mikheev,[a)] Adam P. Kajdos,[a)] Adam J. Hauser, and Susanne Stemmer[b)]
Materials Department, University of California, Santa Barbara, California 93106-5050, USA

(Received 21 October 2012; accepted 7 December 2012; published online 21 December 2012)

We report on the dielectric properties of $Ba_xSr_{1-x}TiO_3$ (BST) films grown by molecular beam epitaxy on epitaxial Pt bottom electrodes. Paraelectric films ($x \lesssim 0.5$) exhibit dielectric losses that are similar to those of BST single crystals and ceramics. Films with device quality factors greater than 1000 and electric field tunabilities exceeding 1:5 are demonstrated. The results provide evidence for the importance of stoichiometry control and the use of a non-energetic deposition technique for achieving high figures of merit of tunable devices with BST thin films. © *2012 American Institute of Physics*. [http://dx.doi.org/10.1063/1.4773034]

The perovskite $Ba_xSr_{1-x}TiO_3$ (BST) is a prototype electric field tunable dielectric that has attracted considerable interest for applications in microwave devices,[1–3] due to its potential to combine low dielectric loss with high tunability. Low losses have been demonstrated for bulk BST ceramics and single crystals.[4–8] Thin film parallel-plate capacitor structures with metal bottom electrodes allow for the application of high fields for high tunabilities. BST films have been grown by pulsed laser deposition, sputtering, metal-organic vapor deposition, and solution methods. It has, however, proved challenging to develop BST thin films that achieve low losses and high tunabilities simultaneously. The best reported BST film quality factors ($Q = 1/\tan\delta$, where $\tan\delta$ is the dielectric loss tangent) are no greater than $\sim$200,[9–14] which is an order of magnitude below Q of $\sim 10^3$ of bulk BST.[5] Furthermore, films with high tunability tend to have high losses,[9,10] which results in low figures of merit.[15] Low dielectric losses have been achieved for $SrTiO_3$ films ($Q \sim 300$),[16] but the room temperature tunability of $SrTiO_3$ is low. Below 200 K, a tunability of $n \sim 2$ combined with low loss ($Q \sim 1000$) has been demonstrated for $SrTiO_3$.[17] Here, n is defined as $n(E) = \varepsilon_r(0)/\varepsilon_r(E)$, where $\varepsilon_r(0)$ is the relative dielectric permittivity at zero field, and $\varepsilon_r(E)$ the permittivity at a given electric field E.

The high dielectric losses of BST thin films have been attributed to poor stoichiometry control,[9,10,16] extended defects due to the growth on mismatched substrates,[15] and point defects from energetic deposition. Control of the BST microstructure is more challenging for growth on metal bottom electrodes than on closely lattice matched perovskite substrates.[18] Oxide molecular beam epitaxy (MBE) allows for low point defect densities, because it is a high-purity, low energetic deposition technique. Strained $SrTiO_3$ films grown by MBE have been shown to exhibit high tunabilities, but also large losses ($Q < 100$).[19] MBE-grown BST films have been reported,[20,21] but have thus far not exhibited improved properties relative to those deposited by other techniques. Here, we report on the dielectric properties of BST films grown by hybrid oxide MBE, a method which has previously been shown to allow for excellent stoichiometry control[22] and low defect densities[23,24] for $SrTiO_3$ films. Films are grown on Pt bottom electrodes to form parallel-plate capacitor structures, which are shown to combine high dielectric tunabilities with Q factors comparable to those of bulk BST.

Epitaxial, 100-nm thick Pt bottom electrodes were grown on (001) $SrTiO_3$ single crystals by DC magnetron sputtering at 825 °C using 10 mTorr Ar sputter gas pressure.[25] Pt grows in cube-on-cube epitaxial orientation on $SrTiO_3$.[25] Pt films were post-growth annealed at 1000 °C for 10 min in oxygen. BST films were grown by MBE (GEN 930 Veeco instrument), using solid source effusion cells for supplying Ba and Sr and a metal organic precursor for Ti (titanium tetra isopropoxide or TTIP), i.e., the hybrid approach used previously for $SrTiO_3$, described elsewhere.[26] All films were grown at a substrate temperature of 750 °C (thermocouple reading). The (Ba + Sr)/Ti (A/B site) stoichiometry was optimized using a calibration growth series on bare $SrTiO_3$. The out-of-plane lattice parameter of BST at each targeted composition was determined as a function of the TTIP beam equivalent pressure (BEP) during growth, using 2θ-ω high-resolution XRD scans of the 002 reflections (Philips X'PERT Panalytical MRD Pro Thin-Film Diffractometer). As noted previously for $SrTiO_3$, the smallest lattice parameter corresponds to A/B site stoichiometry.[22,26] Also similar to $SrTiO_3$,[26] films grown under A/B site stoichiometric conditions exhibited c(4×4) surface reconstructions in *in situ* reflection high-energy electron diffraction. The (Ba + Sr)/Ti calibration was carried out for different Ba/Sr ratios, which were obtained by fixing the Ba cell temperature and adjusting the Sr BEP. Approximately 300 nm thick BST films were then grown on Pt/$SrTiO_3$. Rutherford backscattering spectrometry confirmed that the three different $Ba_xSr_{1-x}TiO_3$ compositions in this study were $x = 0.19$, 0.35, and 0.46. Parallel-plate capacitors were fabricated using a two-step mask process. In the first step, the active capacitor mesa was defined by wet etching in 1:20 diluted trace metal grade HF. A lift-off process was used to pattern 100-nm thick, $45 \times 45\ \mu m^2$ top Pt electrodes, which were deposited by electron beam evaporation. A post-processing 20 min anneal in oxygen was carried out at 800 °C. Dielectric characterization was performed using a Cascade Microtech probe station,

[a)]E. Mikheev and A. P. Kajdos contributed equally to this work.
[b)]Email: stemmer@mrl.ucsb.edu.

 © 2012 American Institute of Physics

GGB 100-μm GSG probes and an HP 4294 A impedance analyzer with a 500 mV oscillation voltage. The large Q values reported in this study can generally be measured less accurately than the smaller Q of typical BST films. The frequency-averaged (10^5–10^6 Hz) values, Q_{av}, of the three films in this study are 140, 1130, and 4350 (see below). These values are subject to an instrument accuracy of 0.075% in the loss tangent (tan δ), giving the following ranges for the different Q_{av}: $140 < Q < 160$ ($Q_{av} = 140$), $610 < Q < 7210$ ($Q_{av} = 1130$), and $1020 < Q$ ($Q_{av} = 4350$).[27]

Figure 1 shows high-resolution XRD 2θ-ω scans of the BST/Pt/$SrTiO_3$ samples with the three different BST compositions. The BST films are predominantly (001) cube-on-cube oriented (as also confirmed in XRD phi-scans), but smaller amounts of BST and Pt (111) and (110) grains were also detected in wide-angle scans (inset in Fig. 1). The thickness fringes are due to the bottom Pt layer, and indicate a smooth growth surface for BST. The BST out-of-plane lattice parameter increases with Ba content. Off-axis measurements of 103 reflections of BST indicated that the films are relaxed, i.e., the in-plane lattice plane spacing is similar to the out-of-plane BST spacing within 0.05%.

Figure 2 shows the dielectric permittivity, ε_r, and the device quality factor Q as a function of frequency. A lower Q at low frequencies is commonly observed and is due to DC leakage.[28] At frequencies above $\sim 10^4$ Hz, Q is dominated by BST loss.[28] BST films with $x = 0.19$ and 0.35 exhibit Q values > 1000. An inverse correlation between Q and permittivity is typical for BST. Several loss mechanisms, both intrinsic and extrinsic, such as charged defects, contribute to the loss proportionally to the permittivity of the material.[1] The drop in Q for the $x = 0.46$ film is due to the film being within or near the ferroelectric phase transition, as evidenced by weak hysteresis in capacitance-voltage measurements, which causes additional loss mechanisms (for example due to domain walls). We note that the ferroelectric phase transition of thin films is typically shifted to higher temperatures relative to bulk.[29] The BST film with $x = 0.19$ exhibits sharp oscillations in Q, which were also observed in other BST films with Qs > 1000, and which were reproducible and independent of the specific instrument used. Further studies are needed to clarify their origin. As an independent confirmation of the high Q values, the capacitance data as a function of frequency were fit to an universal relaxation law, which allows estimating Q via the Kramers-Kronig relation.[30] For the BST films with $x = 0.19$ and 0.35, Q values of $\sim$4000 and $\sim$2000 were obtained by this method.

Figure 3 compares the device Qs in this study (averaged over 10^5–10^6 Hz) with those of the best Qs for single crystal, bulk ceramics, and thin films reported in the literature, as a function of the Ba/Sr ratio. A general trend of decreasing Q with increasing permittivity (Ba content) is observed. The

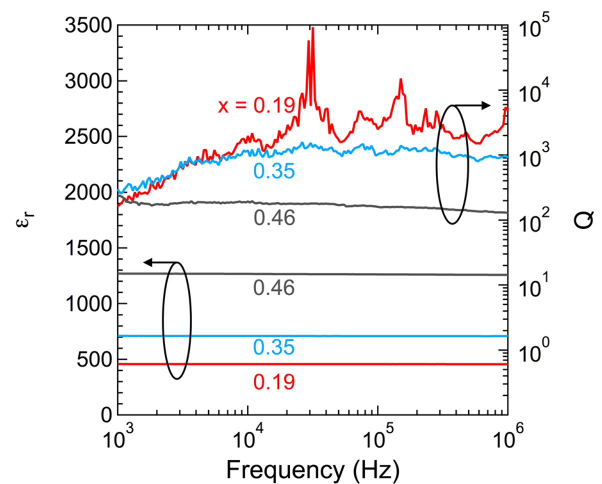

FIG. 2. Dielectric permittivity (left axis) and device quality factor Q (right axis) as a function of frequency for samples with BST films with different Ba concentrations ($x = 0.19$, 0.35, and 0.46). The measured capacitances (at 1 MHz) for the three films were 25.44 pF ($x = 0.19$), 83.82 pF ($x = 0.35$), and 48.19 pF ($x = 0.46$) and their thicknesses ranged from 260 to 300 nm.

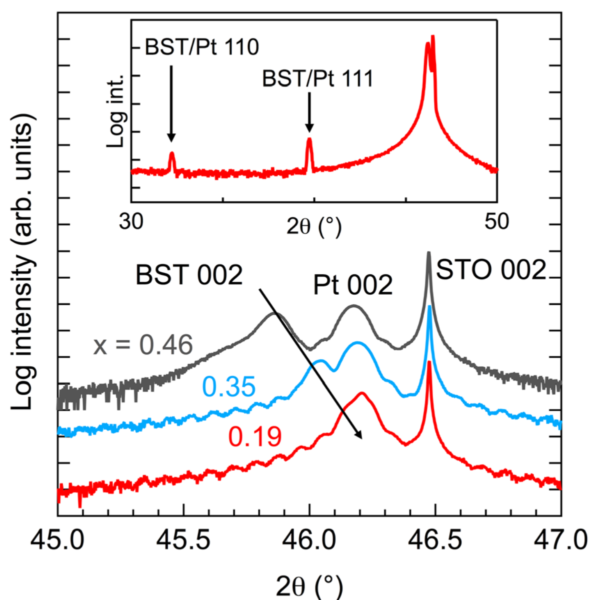

FIG. 1. High-resolution XRD 2θ-ω spectra near the 002 reflection of BST films and $SrTiO_3$ substrates for BST/Pt/$SrTiO_3$ samples and BST films with different Ba concentrations ($x = 0.19$, 0.35, and 0.46). The inset shows a wide-angle scan for $x = 0.19$ and the presence of small amounts of (011) and (111) oriented grains (see corresponding reflections).

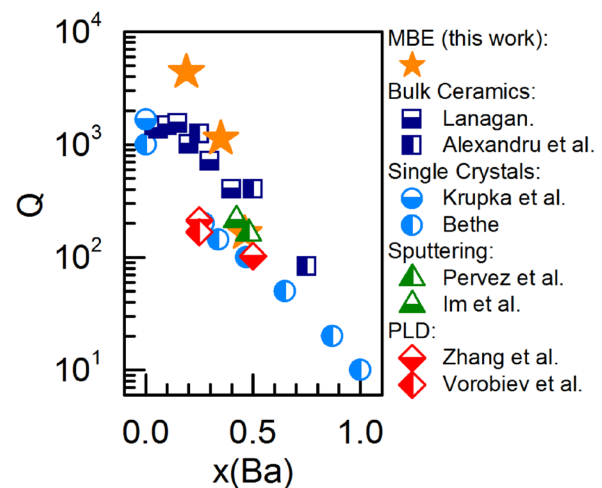

FIG. 3. Comparison of device quality factor Q as a function of Ba content x in BST films, single crystals, and ceramics at zero bias. The literature data are from Lanagan (Ref. 5), Alexandru *et al.* (Ref. 8), Bethe (Ref. 4), Krupka *et al.* (Ref. 33), Im *et al.* (Ref. 9), Pervez *et al.* (Ref. 10), Vorobiev *et al.* (Ref. 11), and Zhang *et al.* (Ref. 12).

paraelectric MBE films show Qs that are equal or greater than those of bulk ceramic and single crystals (even when considering the error margins given above), and an order of magnitude greater than reported thin films. The results show that to minimize losses, control of point defect densities and stoichiometry, as afforded by hybrid MBE, are essential. Conversely, grain boundaries [between (001) and (110)/(111) oriented grains] and dislocations [at low angle grain boundaries between (001) oriented grains], which are present in the MBE films, appear to be less detrimental in terms of achieving low losses.

Figure 4(a) shows the permittivity as a function of E at 1 MHz and the inset shows $n(E)$. The tunability increases with zero-field permittivity, as expected from Landau theory[1] and exceeds 5:1 for the film with $x = 0.35$. Figure 4(b) shows the electric field dependence of Q. The Qs of the paraelectric films are highest at zero field and show a slight drop at small fields. This initial drop in Q with field may be due to the onset of quasi-Debye loss, which is an intrinsic loss mechanism that appears in centrosymmetric materials (i.e., paraelectric BST) when an applied electric field breaks the symmetry.[1] It is not observed in higher loss films in the literature, probably because extrinsic (defect-related) mechanisms dominate the loss in these films—for these mechanisms, the suppression of the dielectric permittivity with field causes a reduction of losses, and an increase in Q with small fields is typically observed. The degradation in Q with higher fields is likely due to increase in leakage and onset of (soft) dielectric breakdown. BST films with lower permittivity (low Ba content) have higher breakdown strengths, and can be biased to higher fields. The inverse correlation between permittivity and breakdown strength is observed in many dielectric materials.[31]

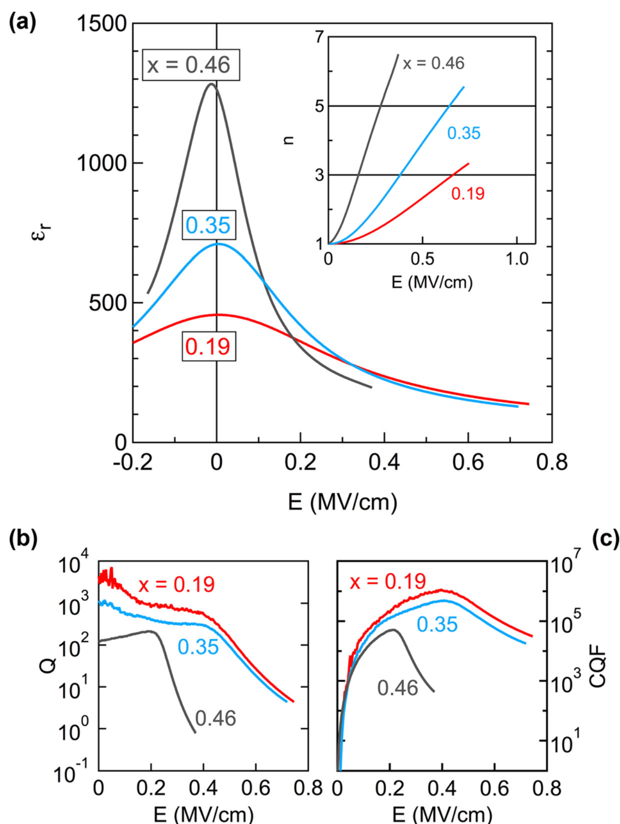

FIG. 4. (a) Field dependent permittivity for samples with BST films with different Ba concentrations ($x = 0.19$, 0.35, and 0.46). The inset shows the tunability as a function of field, $n(E)$. (b,c) Field dependence of the quality factor Q (b), and of the commutation quality factor (c).

A suitable figure of merit for tunable dielectrics is the commutation quality factor as a function of electric field, CQF(E),[32]

$$\mathrm{CQF}(E) = \frac{(n(E)-1)^2}{n(E)} Q(E)Q(0), \tag{1}$$

where $Q(E)$ is the quality factor at the applied electric field and $Q(0)$ is the quality factor at zero bias. Figure 4 shows that the maximum values for CQF(E) are 1×10^6, 5×10^5, and 5×10^4, respectively, for the films with $x = 0.19$, 0.35, and 0.46. These CQF values compare favorably to typical values of 10^1 to 10^4 reported in the literature (for a compilation of literature values and references, see Ref. 15). The large CQFs in this study are due to the combination of very low losses and high tunabilities. Other figures of merit that have been used in the literature include $Q(0)n_r$, where n_r is the relative tunability at the maximum applied field, or $n_r = 1 - n^{-1}$. The films in this study exhibit $Q(0)n_r$ values of 3020 and 830 for $x = 0.19$ and 0.35, respectively, exceeding previously reported values for BST (140, see Ref. 10). We note that reported literature values of figures of merit for tunable dielectrics, including those tabulated in Ref. 15, span a wide range of frequencies. The intrinsic BST Q-factor is, however, not strongly frequency dependent between 1 MHz and 1 GHz.[13] At microwave frequencies, losses are dominated by extrinsic contributions, such as from the series resistance from the electrodes, which makes an extraction of the BST Q-factor challenging.[28]

In summary, we have shown that stoichiometry control and low point defect densities, as afforded by hybrid MBE, allow for high figures of merit of field-tunable BST films. MBE also allows for tuning the Ba:Sr ratio to adjust tunability and loss to meet the needs of a specific application, and the hybrid MBE technique enables easy scaling of growth rates for the deposition of thick films.[26] These films should have excellent potential for future high-performance tunable RF devices and are of sufficient quality to investigate intrinsic loss mechanisms, such as quasi-Debye losses. Future studies should address the properties at microwave frequencies.

The authors thank Alexander Tagantsev, Bob York, and Chris Elsass for discussions, George Saddik for help with processing and measurements, and acknowledge support for this work by Northrop Grumman through the ONR Chip Scale Channelizer Program. E.M. was supported by an AFSOR MURI program (Grant number FA9550-12-1-0038) and A.J.H. by an Elings fellowship. This work made use of the UCSB MRL facilities, which are supported by the MRSEC Program of NSF (award number DMR 1121053) and the UCSB nanofabrication facility, which is part of the NSF-funded NNIN network.

[1] A. K. Tagantsev, V. O. Sherman, K. F. Astafiev, J. Venkatesh, and N. Setter, J. Electroceram. **11**, 5 (2003).
[2] P. Bao, T. J. Jackson, X. Wang, and M. J. Lancaster, J. Phys. D **41**, 063001 (2008).

[3]L. B. Kong, S. Li, T. S. Zhang, J. W. Zhai, F. Y. C. Boey, and J. Ma, Prog. Mater. Sci. **55**, 840 (2010).
[4]K. Bethe, Philips Res. Rep. Suppl 2, 1 (1970).
[5]M. T. Lanagan, Microwave dielectric properties of antiferroelectric lead zirconate, Ph.D. dissertation (The Pennsylvania State University, 1987).
[6]O. G. Vendik, E. K. Hollmann, A. B. Kozyrev, and A. M. Prudan, J. Supercond. **12**, 325 (1999).
[7]D. Garcia, R. Y. Guo, and A. S. Bhalla, Ferroelectr. Lett. Sect. **27**, 137 (2000).
[8]H. V. Alexandru, C. Berbecaru, F. Stanculescu, A. Ioachim, M. G. Banciu, M. I. Toacsen, L. Nedelcu, D. Ghetu, and G. Stoica, Mater. Sci. Eng. B **118**, 92 (2005).
[9]J. Im, O. Auciello, P. K. Baumann, S. K. Streiffer, D. Y. Kaufman, and A. R. Krauss, Appl. Phys. Lett. **76**, 625 (2000).
[10]N. K. Pervez, P. J. Hansen, and R. A. York, Appl. Phys. Lett. **85**, 4451 (2004).
[11]A. Vorobiev, P. Rundqvist, K. Khamchane, and S. Gevorgian, J. Appl. Phys. **96**, 4642 (2004).
[12]X. Y. Zhang, P. Wang, S. Sheng, F. Xu, and C. K. Ong, J. Appl. Phys. **104**, 124110 (2008).
[13]A. Tombak, J. P. Maria, F. Ayguavives, Z. Jin, G. T. Stauf, A. I. Kingon, and A. Mortazawi, IEEE Microw. Wirel. Compon. Lett. **12**, 3 (2002).
[14]M. W. Cole, R. C. Toonen, M. Ivill, S. G. Hirsch, E. Ngo, and C. Hubbard, J. Appl. Phys. **110**, 124105 (2011).
[15]T. J. Jackson and I. P. Jones, J. Mater. Sci. **44**, 5288 (2009).
[16]T. R. Taylor, P. J. Hansen, N. Pervez, B. Acikel, R. A. York, and J. S. Speck, J. Appl. Phys. **94**, 3390 (2003).
[17]H. C. Li, W. D. Si, A. D. West, and X. X. Xi, Appl. Phys. Lett. **73**, 464 (1998).
[18]S. Schmidt, J. W. Lu, S. P. Keane, L. D. Bregante, D. O. Klenov, and S. Stemmer, J. Am. Ceram. Soc. **88**, 789 (2005).
[19]J. H. Haeni, P. Irvin, W. Chang, R. Uecker, P. Reiche, Y. L. Li, S. Choudhury, W. Tian, M. E. Hawley, B. Craigo *et al.*, Nature **430**, 758 (2004).
[20]H. Li, J. Finder, Y. Liang, R. Gregory, and W. Qin, Appl. Phys. Lett. **87**, 072905 (2005).
[21]P. Fisher, M. Skowronski, P. A. Salvador, M. Snyder, J. Xu, M. Lanagan, O. Maksimov, and V. D. Heydemann, Mater. Res. Soc. Proc. **966**, 0966 (2006).
[22]B. Jalan, P. Moetakef, and S. Stemmer, Appl. Phys. Lett. **95**, 032906 (2009).
[23]J. Son, P. Moetakef, B. Jalan, O. Bierwagen, N. J. Wright, R. Engel-Herbert, and S. Stemmer, Nat. Mater. **9**, 482 (2010).
[24]D. J. Keeble, B. Jalan, L. Ravelli, W. Egger, G. Kanda, and S. Stemmer, Appl. Phys. Lett. **99**, 232905 (2011).
[25]J. Son, J. Cagnon, and S. Stemmer, J. Appl. Phys. **106**, 043525 (2009).
[26]B. Jalan, R. Engel-Herbert, N. J. Wright, and S. Stemmer, J. Vac. Sci. Technol. A **27**, 461 (2009).
[27]*Agilent 4294A Precision Impedance Analyzer. 40 Hz to 110 MHz. Data Sheet* (Agilent Technologies, 2008).
[28]R. A. York, in *Multifunctional Adaptive Microwave Circuits and Systems*, edited by M. Steer and W. D. Palmer (SciTech, 2009).
[29]N. A. Pertsev, A. G. Zembilgotov, and A. K. Tagantsev, Phys. Rev. Lett. **80**, 1988 (1998).
[30]N. K. Pervez, J. Park, J. W. Lu, S. Stemmer, and R. A. York, Integr. Ferroelectr. **77**, 87 (2005).
[31]J. McPherson, J. Y. Kim, A. Shanware, and H. Mogul, Appl. Phys. Lett. **82**, 2121 (2003).
[32]I. B. Vendik, O. G. Vendik, and E. L. Kollberg, IEEE Trans. Microw. Theory Tech. **48**, 802 (2000).
[33]J. Krupka, R. G. Geyer, M. Kuhn, and J. H. Hinken, IEEE Trans. Microw. Theory Tech. **42**, 1886 (1994).